Publishing Excellence
Inspiring Progress

ISSN: 0000-0000 www.aristonpubs.com/journal/science-of-optics-and-photonics https://doi.org/10.69626/sop.2026.0044

RESEARCH ARTICLE

Novel Combined Strategy to Obtain More Efficiency in the CdTe – Thin Film Solar Cell using SCAPS – 1D

Bishal Hazarika[1], K Bijayata Singha[1], Sagar Bhattarai[2*]

ABSTRACT: In this study, the photovoltaic performance of CdTe based thin-film solar cells with an IGZO electron transport layer (ETL) and Cu_2O hole transport layer (HTL) is studied through SCAPS-1D simulation software. In order to improve the performance of the cell, variations in absorber thickness, defect densities in ETL (IGZO) and HTL(Cu_2O), and different choices for front and rear contacts were examined. It is clear from the simulation results that variation in any of these factors plays a vital role in improving the power conversion efficiency (PCE), open-circuit voltage (V_{oc}), short-circuit current density (J_{sc}), and fill factor (FF). The most significant factor in improving efficiency turned out to be the absorber's defect density, followed by selecting good contact materials. The maximum efficiency achieved via simulations gives values of 18.84 mA/cm2 for J_{sc} . 1.35 V for V_{oc} , 90.46% for FF, and PCE of 23.01% under AM1.5G radiation.

Keywords: : CdTe; Thin Film Solar Cell; Photo-Voltaic(PV); SCAPS-1D; Defect Density (N_t); Absorber Layer; Power Conversion Efficiency (PCE); Electron Transport Layer (ETL); Hole Transport Layer (HTL); Band Alignment.

Received: 21 May 2026; Revised: 02 August 2026; Accepted: 12 August 2026; Published Online: 29 August 2026

1. INTRODUCTION

With the rise in the world's energy demand along with the increasing threat posed by global warming and carbon emissions, there has been an increased emphasis on sustainable and low-carbon energy sources [1]. Of all the renewable energy sources that are present, the energy from the sun is considered one of the best choices due to its plentifulness, environmental friendliness, and sustainability [1, 2]. The PV technology, which converts the sun's rays directly into energy, has seen rapid advancements through constant development in terms of material composition, design architecture, and fabrication, resulting in the enhancement of power conversion efficiency (PCE) and reduction in fabrication costs [2, 3]. Nonetheless, additional enhancements in terms of PCE, stability, and fabrication cost still need to be made in order to enable the widespread use of PV technology [1, 2]. Among various PV technologies, thin film PVs have gained much popularity due to the requirement of small amounts of semiconductor materials, ability to fabricate large areas, and possibility of low-cost production [4]. Several thin film absorber materials such as a-Si, CIGS, CdTe, and thin film materials of the next generation exhibit superior photovoltaic properties [4, 5]. Out of these, CdTe continues to be one of the most advanced thin film technologies on account of its high value of optical absorption, appropriate band gap, and scalability of its manufacturing process [5]. This makes it a good choice for further improvements of photovoltaic properties. Although considerable progress has been achieved in CdTe solar cells, device performance is still influenced by carrier recombination, defect states, and interface-related losses, which can reduce charge extraction and limit the open-circuit voltage (V_{OC}), fill factor (FF), and overall power conversion

[1] Department of Physics, Cotton University, Panbazar, Guwahati 781001, Assam, India
[2] Technology Innovation Hub, Indian Institute of Technology Guwahati, Guwahati 781039, Assam, India

* Author to whom correspondence should be addressed: sagarbhattarai012@gmail.com (S. Bhattarai)

© Ariston Publications 2026. All rights reserved.

efficiency [6]. Therefore, optimizing both the absorber layer and charge transport layers is essential for minimizing recombination losses and improving carrier collection. Previous studies have demonstrated that defect density, interface quality, and transport-layer properties strongly influence photovoltaic device performance [6, 7]. There are numerous transport materials studied for their use in the photovoltaic devices among which cuprous oxide (Cu_2O) gained much popularity as a hole transport material due to its wide bandgap, optical transparency, p-type conductivity, and appropriate electronic properties [7]. In the same way, indium gallium zinc oxide (IGZO) became quite promising as a transparent oxide semiconductor thanks to its high mobility, optical transparency, wide bandgap, and chemical stability that made it suitable for electron transport applications [8]. Thus, using Cu_2O and IGZO together will result in improving charge separation and carrier transport with minimal interface losses, which should positively affect CdTe solar cell performance.

Numerical simulation has turned into an important tool for studying and optimizing the photovoltaic devices since it allows one to examine the properties of materials and devices parameters before conducting experiments [3]. SCAPS-1D is one of such simulation software widely used in modeling thin film solar cells due to its ability to study carrier transport, recombination processes, and current-voltage characteristics depending on different conditions [9, 10]. Motivated by these considerations, the present study numerically investigates a Front Contact/Cu_2O/CdTe/IGZO/Back Contact thin-film solar cell using SCAPS-1D. The influence of absorber thickness, transport-layer thickness, defect density, series resistance, shunt resistance, and operating temperature on photovoltaic performance is systematically examined. Furthermore, current density-voltage (J–V), quantum efficiency (QE), capacitance-voltage (C–V), and heatmap analyses are employed to evaluate charge transport behaviour and identify optimum operating conditions. The findings of this work provide useful insights into the optimization of efficient and stable CdTe thin-film solar cells.

2. SIMULATION METHODOLOGY AND CELL ARCHITECTURE

In our study, numerical device simulations are done using the Solar Cell Capacitance Simulator (SCAPS-1D). SCAPS-1D allows us for numerical modelling of layered photovoltaic structures by solving Poisson's and Carrier continuity equations which are under steady state conditions [3, 9]. The proposed solar cell model is based on the heterojunction structure defined as:Front Contact / IGZO/ CdTe / Cu_2O / Back Contact. In this architecture, Cadmium Telluride (CdTe) is acting as the primary absorber layer owing to its optimal direct bandgap (1.7 eV) and high optical absorption coefficient. This allows efficient photon capture within a thin film [11]. Cuprous Oxide (Cu_2O) acts as the Hole Transport Layer (HTL) at the back contact. The p-type semiconductor characteristics and suitable valence band offset of Cu_2O facilitate effective hole extraction and serve as an electron-blocking layer to suppress back-surface recombination [12, 13]. Indium Gallium Zinc Oxide (IGZO) acts as the n-type Electron Transport Layer (ETL) / window layer at the front contact. IGZO has a wide direct bandgap (3.05 ev) and high electron mobility. Because of this IGZO minimizes parasitic optical absorption losses in the high-energy spectrum while promoting efficient electron transport to the front contact [14, 15]. This configuration ensures that photogenerated electrons migrate toward the front contact via IGZO while photogenerated holes are extracted at the back contact via , enabling effective charge separation and reducing recombination losses. All layers' physical parameters, including thickness, bandgap, doping density, carrier mobility, and defect density, are set based on literature and optimized in SCAPS-1D to enhance device performance. The standard AM1.5G illumination with an intensity of 1000 mW/m² is used to simulate the conditions for solar operation. Summary of layer wise input parameters is shown in Table 1. Hence by adjusting absorber and interface defect levels thickness, we can enhance light absorption and generate more electron-hole pairs and achieve better short-circuit current density and power conversion efficiency (PCE) [16].

3. NUMERICAL MODELLING

To get the highest efficiency possible for solar cells it required various computational modelling techniques. Numerical modelling is essential as the cost and time required to fabricate solar cells can become unsuitable [17, 18]. This approach eliminates the need for potentially hazardous experimental investigations of material properties, allowing researchers to simulate and refine the structure digitally. Furthermore, it gives us a systematic framework for evaluating the relative impact of different material parameters on device performance, especially valuable in the rapidly advancing field

 © Ariston Publications 2026. All rights reserved.

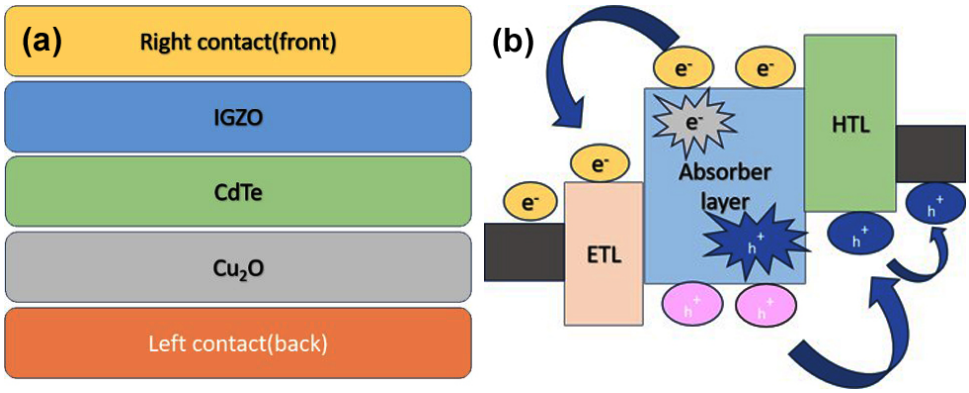

Fig. 1. (a) Structural representation CdTe based thin film solar cell (b) Schematic of energy levels depicting carrier transport in ETL and HTL..

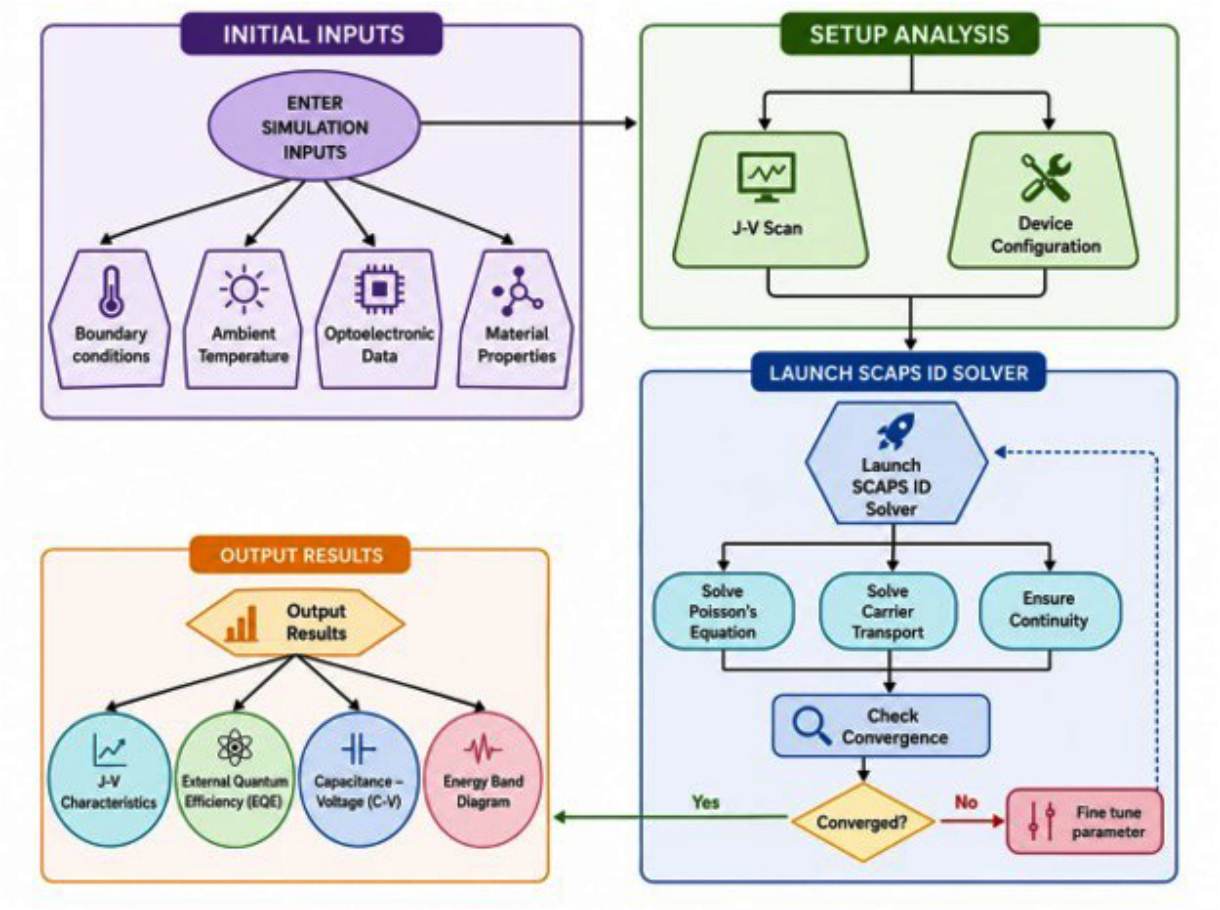

Fig. 2. Graphical representation of the working of SCAPS 1D simulation.

of perovskite solar cells (PSCs) [17]]. SCAPS-1D is a simulation tool developed by Burgelman and colleagues and is widely used to analyze and optimize solar cell structures [3, 9]. These tools enable researchers to study electrical behaviors, including recombination, carrier transport, and energy band alignment, within a one-dimensional framework [18]. The governing equations describe the steady-state behavior of semiconductors under illumination. The Poisson's equation is used to define the relationship between electrostatic potential φ, electric field E, and charge density ρ in a p–n junction, and is expressed as follows [9]:

$$\frac{\partial^2\varphi}{\partial x^2} = -\frac{\partial E}{\partial x} = -\frac{\rho}{\varepsilon_s}$$

$$= -\frac{q}{\varepsilon_s}\left[p - n + N_D^+ - N_A^- \pm N_{\text{def}}(x)\right] \quad (1)$$

© Ariston Publications 2026. All rights reserved.

φ denotes the electrostatic potential, q signifies charge, ε_s indicates the static relative permittivity, and n and p represent electrons and holes, respectively. The characters N_D^+ and N_A^- denote the donor and acceptor densities, respectively, whereas $N_{def}(x)$ represents the defect density of acceptor and donar. [9]

The continuity equations for electrons and holes ensure charge conservation across the device and are given as [9]:

$$-\frac{\partial j_p}{\partial x} + G - U(n,p) = 0 \tag{2}$$

$$\frac{\partial j_p}{\partial x} + G - U(n,p) = 0 \tag{3}$$

The current density equations that describe the movement of carriers via drift and diffusion mechanisms are [9]:

$$j_p = qn\mu_p E - qD_p \frac{\partial p}{\partial x} \tag{4}$$

$$j_n = qn\mu_n E - qD_n \frac{\partial n}{\partial x} \tag{5}$$

Where, μn and μp are the carrier mobilities, q is the electronic charge, and Dn and Dp are the carrier diffusion coefficients [9].

As it can be seen in the flowchart, typical architecture involving solar cells are solved with the help of SCAPS-1D, showing the point of view of user by taking inputs for the problems identified to getting the outputs that can involve multiple steps. SCAPS-1D already includes the basic formulae required for solar cell properties like general recombination rates and current density [3, 9].

4. RESULTS AND DISCUSSIONS

In this section we are going to discuss the outcome of the estimation of the performance characteristics of thin film solar cell based on the absorber CdTe . The hole transport layer (HTL) is Cu_2O, and the electron transport layer (ETL) is IGZO.

4.1 Bandgap analysis of CdTe thin film solar cell

Optimization of the energy band alignment between the absorber material and its neighboring charge transport layers is essential for the efficient operation of CdTe thin film solar cells. Appropriate band alignment at the interfaces is important for optimizing carrier transport and minimizing any losses that can occur due to interfacial recombination [5]. Appropriate conduction band alignment at the interface between the absorber material and the electron transport layer (ETL) ensures a good path for the electron extraction process, whereas appropriate valence band alignment at the absorber and hole transport layer (HTL) interface ensures good hole transport [3]. The energy-band diagram of the simulated thin-film solar cell structure consisting of Cu_2O (HTL)/CdTe (absorber)/IGZO (ETL) is presented in Figure 3. In the proposed configuration, CdTe acts as the active absorber layer with a bandgap of 1.740 eV and is energetically positioned between Cu_2O and IGZO. The electron affinity values considered in the simulation are 3.90 eV for CdTe, 4.160 eV for IGZO, and 3.40 eV for Cu_2O. These electron affinity and bandgap parameters are used to determine the conduction band offset (CBO) and valence band offset (VBO) at the respective interfaces, which strongly influence carrier transport and recombination behaviour within the device [3].

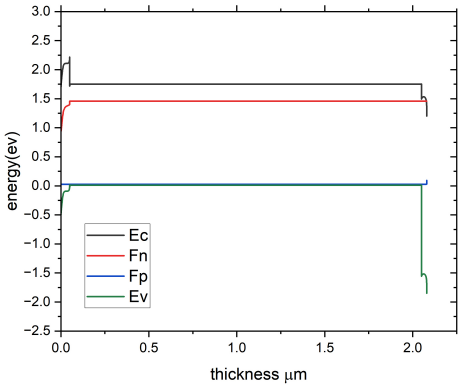

Fig. 3. Illustration of single ETL and HTL CdTe-based thin film solar cell under AM1.5G illuminance.

For CdTe/IGZO interface:

$$\text{CBO} = \chi_{\text{CdTe}} - \chi_{\text{IGZO}} \tag{6}$$

$$\text{VBO} = (\chi_{\text{CdTe}} + E_{g,\text{CdTe}}) - (\chi_{\text{IGZO}} + E_{g,\text{IGZO}}) \tag{7}$$

For Cu_2O/CdTe interface:

$$\text{CBO} = \chi_{Cu_2O} - \chi_{\text{CdTe}} \tag{8}$$

$$\text{VBO} = (\chi_{Cu_2O} + E_{g,Cu_2O}) - (\chi_{\text{CdTe}} + E_{g,\text{CdTe}}) \tag{9}$$

© Ariston Publications 2026. All rights reserved.

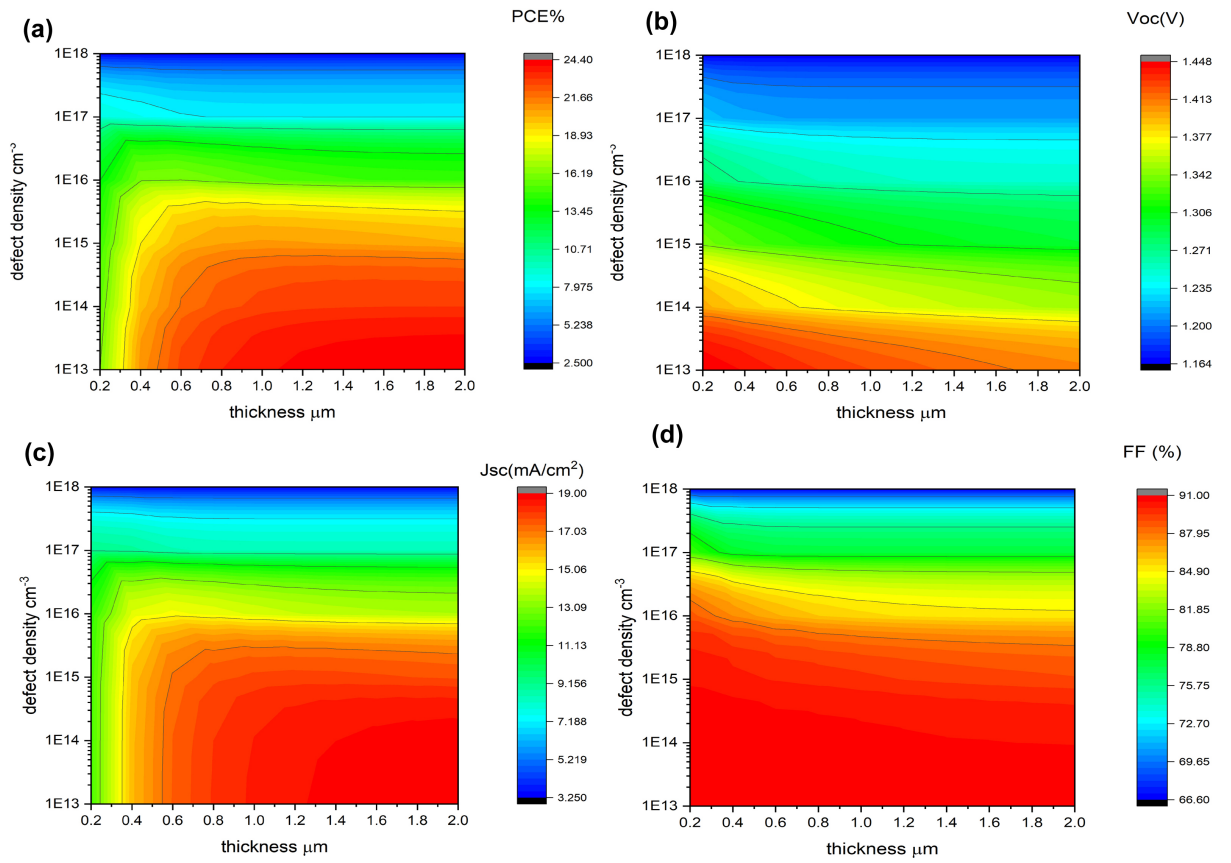

Fig. 4. The performance of the CdTe-based thin film solar cell was evaluated under standard AM1.5G illumination by changing the thickness of the CdTe absorber layer.

The determined offsets are useful in understanding the charge transport property of the suggested device. Suitable conduction band offset at the interface between CdTe and IGZO helps in the efficient extraction of electrons to the ETL and also minimizes the accumulation of electrons at the interface [3, 14]. Just like conduction band, valance band offset at the interface of Cu_2O and CdTe helps in minimizing the chance of back electron transfer and recombination [3, 5].

The choice of Cu_2O and IGZO as the charge transport layers provides desirable electrical and optical properties that help in efficient carrier transport in photovoltaic devices. IGZO has been widely studied as the transparent oxide for use as an electron transport layer owing to its desirable properties such as optically transparent, good electrical properties and ability for efficient electron extraction in photovoltaics [14]. The electric field created in the solar cell is a result of the difference in work functions of the front and back contacts [3].

This study evaluates interface defects in a neutral state at the Cu_2O/CdTe and CdTe/IGZO interfaces. The defect states are generated at an energy position of 0.6 eV higher than the valence band with capture cross-sections of 1×10-19cm² at both interfaces, as illustrated in Table 2. Interface and absorber defect states could serve as recombination sites and decrease the lifetime of the carriers; this impacts the photovoltaic properties [6]. It is thus important to regulate the interface defects to reduce non-radiative recombination [6].

4.2 Impact of active layer thickness on output:

Figure 4a to 4d illustrates the combined influence of CdTe absorber thickness (0.2–2.0 μm) and bulk defect density (10^{13}–10^{18} cm^{-3}) on the photovoltaic performance of the proposed IGZO/CdTe/Cu_2O solar cell. The contour maps indicate that device performance is affected more strongly by defect density than by absorber thickness.

As shown in Figure 4a, the PCE increases rapidly with absorber thickness up to approximately 1 μm, beyond which the contours become nearly horizontal, indicating saturation due to sufficient photon absorption within the CdTe layer. Similar thickness-dependent behaviour has been reported in CdTe-based solar cells, where increasing absorber thickness improves carrier generation until an

© Ariston Publications 2026. All rights reserved.

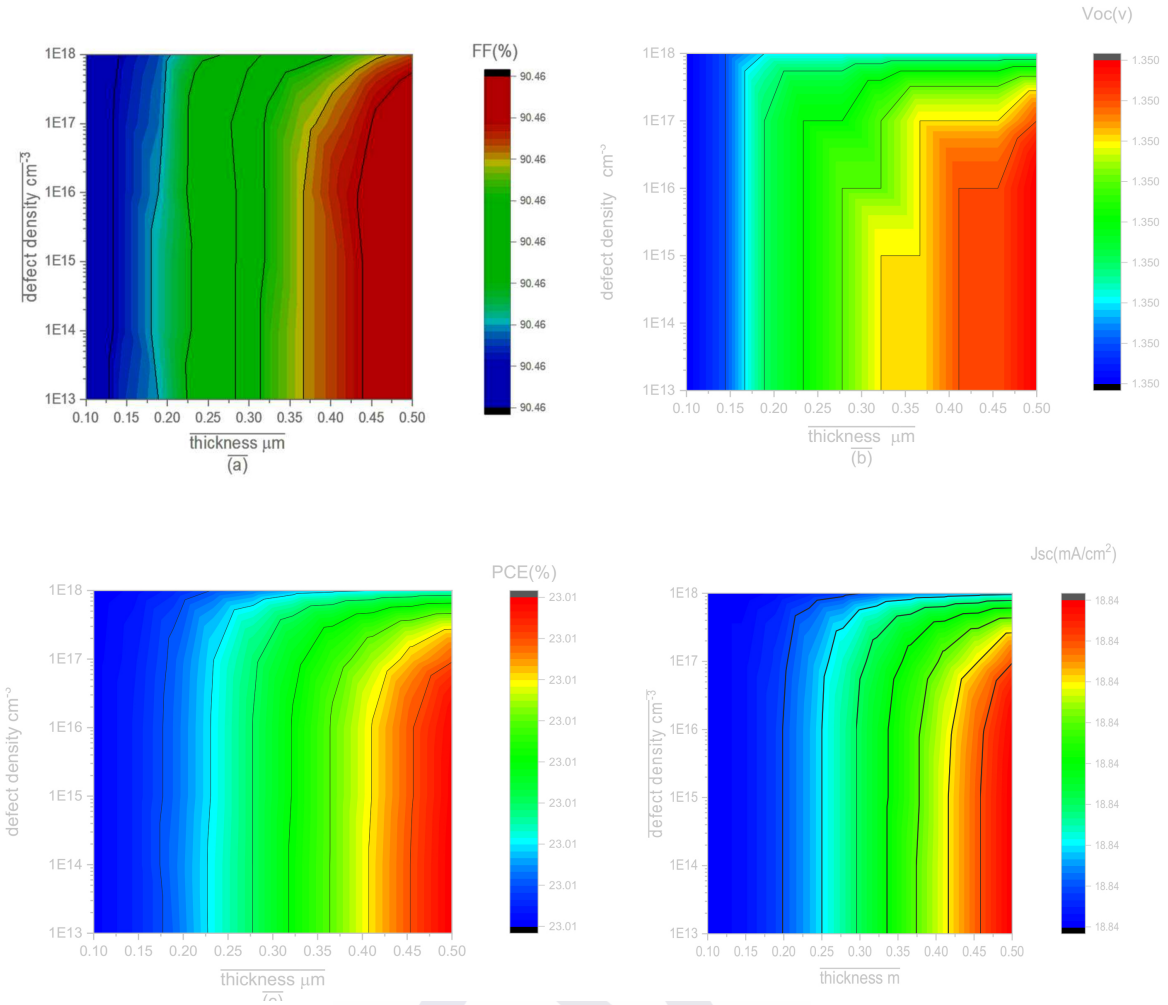

Fig. 5. The PV parameters on the output of the Thin Film Solar Cell under AM1.5G illuminance at different HTL Layer Thickness and defect density.

optimum thickness is reached [19]. The highest efficiency (∼24.4%) is obtained in the low-defect region (10^{13}–10^{14} cm^{-3}), whereas increasing defect density shifts the contours towards lower efficiency values. This reduction is attributed to the formation of defect-assisted recombination centres, which increase carrier losses within the absorber layer [20].

As seen in Figure 4b, the V_{OC} is more dependent on the defect density than the absorber thickness since the contour lines are almost horizontal. In addition, V_{OC} decreases from 1.45 V to 1.17 V as the defect density is increased from 10^{13} to 10^{18} cm^{-3} due to increased recombination and increased carrier losses in the device [20, 21]. J_{sc}, on the other hand, is seen in Figure 4c to increase with absorber thickness before saturation at ∼1 µm since the absorber thickness improves the absorption of photons and carrier generation [19]. The defect density, however, limits the J_{sc} values in all thicknesses as it reduces the carrier lifetime and the collection efficiency due to recombination [20, 21]. In Figure 4d, it is observed that the FFs depend slightly on the absorber thickness while they significantly reduce with an increase in defect density. In particular, the FF reduces from approximately 91% to 69%. This behaviour confirms that the defect states limit the carrier transport and recombination losses, leading to poor charge extraction efficiency [20]. Hence, the contour maps show the optimum range for absorber thickness to be 1 – 1.5 µm and 10^{13} – 10^{14} cm^{-3} for defect density.

4.3 Impact of the HTL thickness and Defect density on outputs.

Once the best absorber thickness is known, then the influence of the HTL material of Cu_2O is studied in order to know how to achieve efficient hole extraction with minimum losses due to recombination. Figure 5a to 5d presents the dependence of FF, V_{oc}, PCE, and J_{sc} on the thickness of Cu_2O and defect density of HTL. The HTL thickness varied between 0.10 and 0.50 µm, while the defect density ranged from 10^{13} to 10^{18} cm^{-3}. As can be seen from the contour plots, the higher Cu_2O thickness leads

 © Ariston Publications 2026. All rights reserved.

Table 1. The employed inputs for the simulated device configuration.

Parameters	Terms	ETL (IGZO) [22]	Absorber Layer (CdTe)	HTL (Cu_2O) [22]
t (μm)	Thickness	0.030	2.00	0.050
E_g (eV)	Bandgap	3.050	1.74	2.2
χ	Electron affinity	4.160	3.9	3.4
ε_r	Relative Permittivity	10	9	7.5
N_c (cm^{-3})	Eff. DoS at CB	5×10^{18}	1×10^{21}	2×10^{19}
N_v (cm^{-3})	Eff. DoS at VB	5×10^{18}	2×10^{20}	1×10^{20}
μ_n (cm^2/Vs)	Electrons Mobility	1.5×10^{1}	2×10^{1}	2×10^{2}
μ_p (cm^2/Vs)	Holes Mobility	1×10^{-1}	1×10^{1}	8.6×10^{3}
N_a (cm^{-3})	Dopant density (Acceptor)	0	1×10^{20}	1×10^{18}
N_d (cm^{-3})	Dopant density (Donor)	1×10^{17}	0	0
N_t (cm^{-3})	Defect Density	1×10^{15}	1×10^{14}	1×10^{15}

Table 2. Input interface defects parameter used in the simulations.

Parameters	Cu_2O/CdTe	CdTe/IGZO
Def. type	Neutral	Neutral
Cap. cross-section of e (cm^2)	1×10^{-19}	1×10^{-19}
Cap. cross-section of h (cm^2)	1×10^{-19}	1×10^{-19}
Energy distributions	Single	Single
Ref. for defect energy level	Above the highest E_V	Above the highest E_V
Energy with respect to ref. (eV)	0.6	0.6
Total density (cm^{-3})	1×10^{10}	1×10^{10}

to the increase in the efficiency of the solar cell. Improvement in terms of thickness is noted for all four characteristics of the device. As the Cu_2O layer becomes thicker, the regions related to higher values of PCE, V_{oc}, J_{sc}, and FF also cover a wider area, with the maximum efficiency being recorded when the thickness is about 0.50 µm. In such a case, the PCE of the cell is around 23.01%, alongside the V_{oc} value of about 1.35 V, J_{sc} value of 18.84 mA cm^{-2}, and FF value close to 90.46%. The improvement in terms of thickness is noted due to the fact that Cu_2O does not serve as an absorber but acts as a hole-selective layer [23].

A different trend is observed when the HTL defect density is increased. Although the optimum thickness remains close to 0.50 µm, the high-performance region becomes progressively smaller as the defect density rises from 10^{13} to 10^{18} cm^{-3}. The contour maps reveal that PCE is the most sensitive parameter, followed by J_{sc} and V_{oc}, while the variation in FF is comparatively moderate. This behaviour indicates that additional defect states promote non-radiative Shockley–Read–Hall recombination, allowing more carriers to recombine before reaching the contacts and thereby reducing the overall conversion efficiency [24]. The interplay between the results from the contour plots indicates that optimizing the electrical characteristics of the HTL layer is as crucial as choosing its thickness. In the considered range, an increase in the Cu_2O thickness is helpful for the carrier extraction, but the effect becomes less pronounced in the case of a high defect density. Consequently, the highest device efficiency is achieved by employing a 0.50 µm Cu_2O layer with low HTL defect density, since in this case charge transport is better and losses due to recombination become smaller. This finding is supported by recent numerical analysis, which demonstrated that transport layer optimization is the most effective at a low defect density [25].

4.4 Combined impact of ETL layer thicknesses and Defect density on the performance of Device

After establishing the optimum hole transport layer, the performance of the IGZO electron transport layer was examined by varying both its thickness and defect density. Rather than influencing each photovoltaic parameter independently, Figure 6a to 6d shows a remarkably similar contour pattern for FF, V_{oc}, PCE, and J_{sc}. In every case, the highest-performing region is confined to the lower-left corner of the contour maps, corresponding to a thin ETL with a low defect density. As either variable increases, this region steadily contracts, indicating that efficient electron extraction depends on the combined optimization of both structural and electrical properties of the transport layer.

This change becomes most evident in the PCE contours. Rather than having the drop in efficiency occur immediately, the contour lines become displaced in the direction of lower efficiencies as the IGZO layer thickens from 0.10 to 0.50 µm. The displacement indicates that increased thickness of the transport layer means higher resistance for electrons, which makes it less efficient for carrier collection.

© Ariston Publications 2026. All rights reserved.

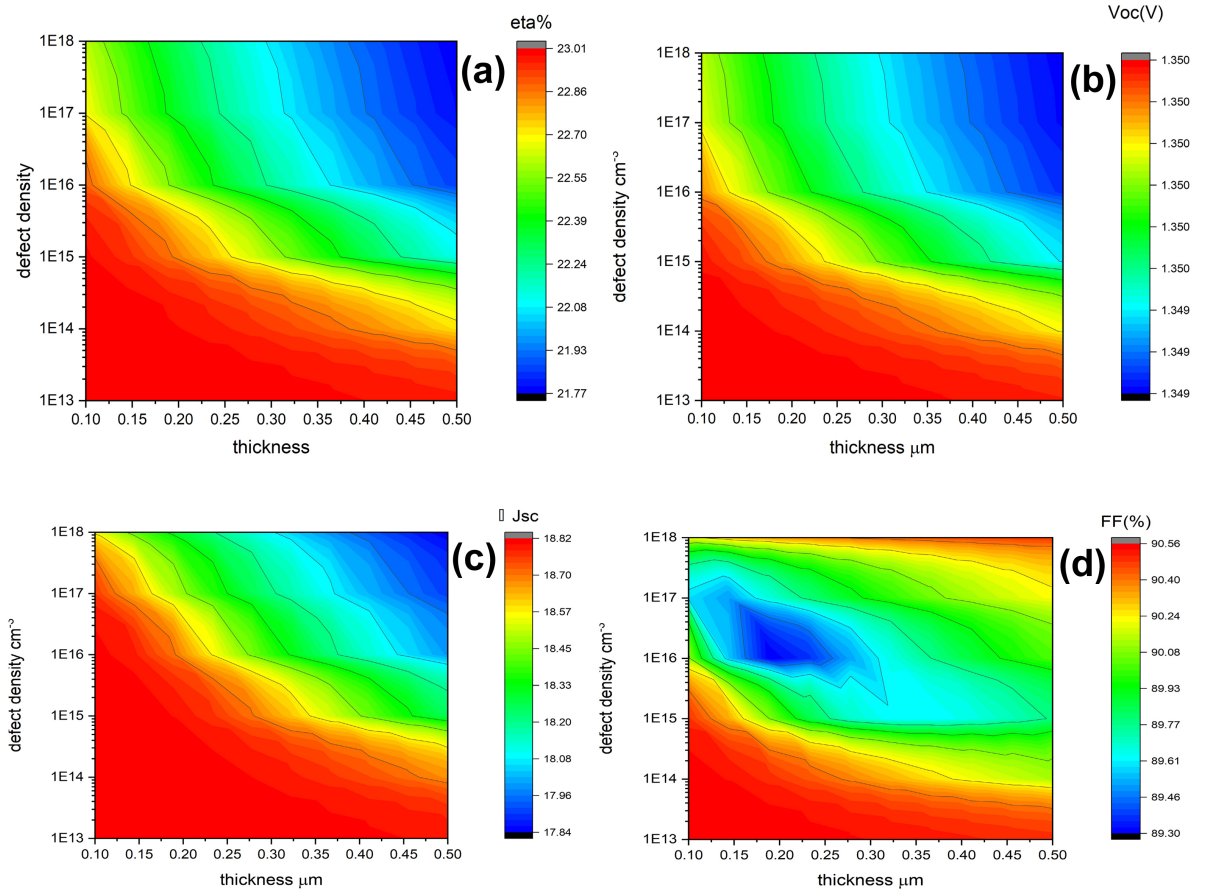

Fig. 6. The PV parameters on the output of the Thin Film Solar Cell under AM1.5G illuminance at different ETL Layer Thickness and defect density.

There is a similar trend seen in the J_{sc} contours, where the drop in current occurs in nearly the same direction as the displacement in efficiency contours. These trends suggest that the cause of the decrease in efficiency is charge collection efficiency, rather than optical absorption [26].

The case is different for V_{oc} and FF. Despite their decreasing trends with the increase in thickness and defects, contour gradients of both V_{oc} and FF are smoother compared to that of PCE. Thus, the electrical properties of the junction remain relatively constant whereas the process of carrier transport becomes increasingly challenging. Due to the rise in the defect density up to 1018 cm^{-3}, the contour lines become more compressed and closer to lower values due to the enhanced trapping of carriers and recombination in the ETL and the interface between the CdTe and IGZO [27].

Taken together, the contour maps suggest that ETL thickness alone does not determine device performance. A thin transport layer is beneficial only when accompanied by good electrical quality, whereas increasing defect density suppresses the advantage gained from thickness optimization. Within the investigated range, the combination of an IGZO thickness of 0.10 µm and a defect density of 10^{13} cm^{-3} provides the most favorable operating condition, producing the highest V_{oc}, J_{sc}, FF, and PCE. Similar conclusions have been reported in recent numerical optimization studies of CdTe solar cells, where reducing transport-layer resistance together with interface recombination led to significant improvements in device efficiency [25].

4.5 Combined impact of the series-shunt resistances on outputs:

The effects of series resistance (R_s) and shunt resistance (R_{sh}) on the Front Contact/Cu_2O/CdTe/IGZO/Back Contact solar cell are shown in Figure 7a to 7d. It can be seen from the contour plots that the optimal device parameters are achieved for low Rs (0–0.5 Ω·cm^2) and high R_{sh} (10^8–10^{10} Ω·cm^2), when all the four parameters of interest (V_{OC}, J_{SC}, FF, and PCE) attain maximum values. Similar results have been obtained in SCAPS-based optimization analysis of CdTe solar cells [28].

 © Ariston Publications 2026. All rights reserved.

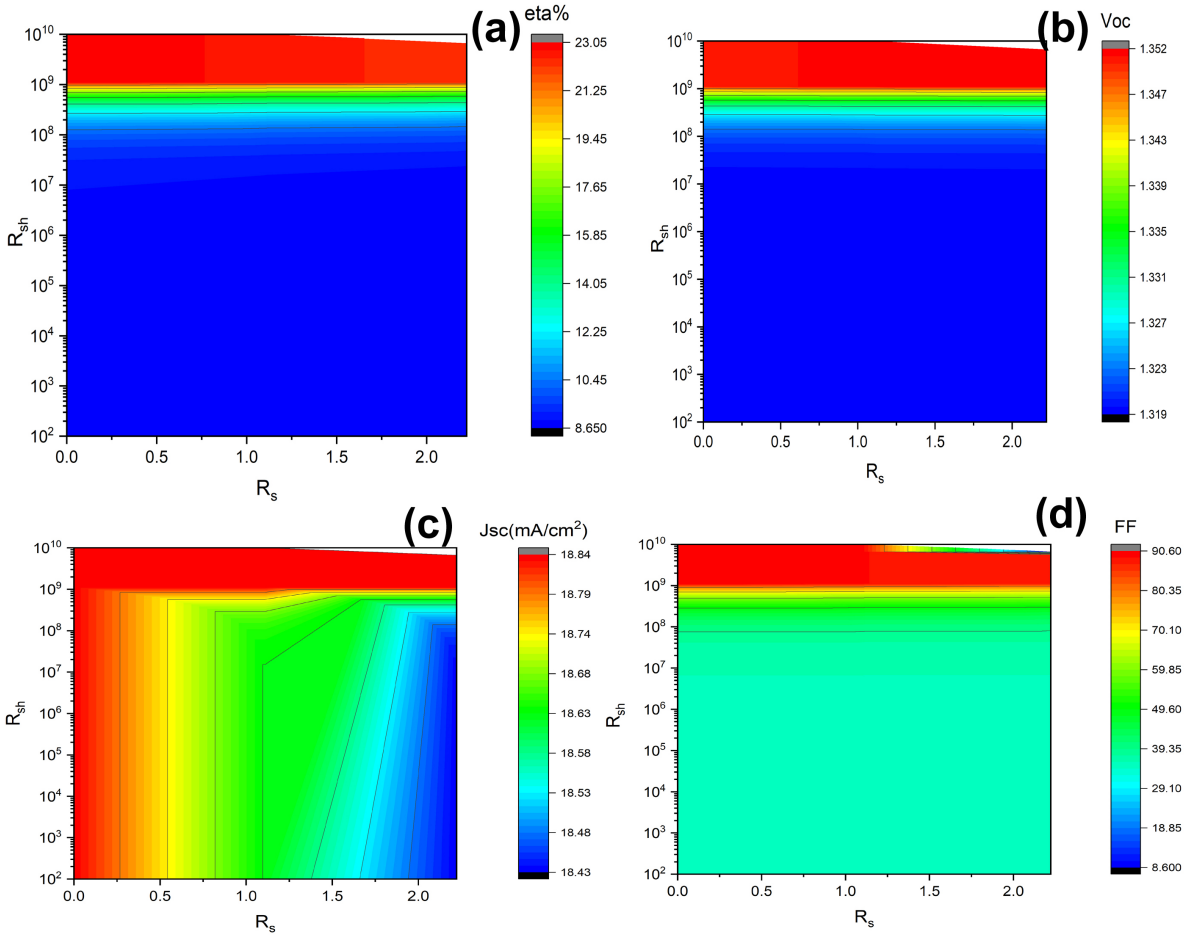

Fig. 7. The PV parameters on the output of the Thin Film Solar Cell with respect to series and shunt resistances.

The V_{OC} contour in Figure 7a is rather horizontal, which means that the V_{OC} parameter is predominantly affected by R_{sh}. An increase in shunt resistance results in a decrease in leakage currents, and, therefore, V_{OC} gradually rises up to a certain value of R_{sh}, above which the improvement becomes insignificant [10]. In turn, the contours in Figure 7d are almost vertical, and this means that the J_{SC} parameter is mostly dependent on Rs. Increased series resistance leads to a loss of carriers during transport, which causes a decrease in J_{SC} [18].

The distribution contours of FF and PCE shown in Figure 7b and Fig. Figure 7c are an outcome of the joint effect of the two resistance parameters. The two parameters attain their highest values in the range of low Rs and high R_{sh}. On the other hand, increasing the value of Rs or reducing the value of R_{sh} leads to degradation of the device performance [28].

4.6 Dependence of Temperature in performance of the Device:

Temperature is another important factor which has a strong effect on the performance of thin film CdTe solar cell [29]. In the case of this study CdTe based solar cell is examined under AM1. 5G illumination under the influence of temperature at 300–380 K. Figure 8 shows that when temperature is increased, the open-circuit voltage (V_{OC}), power conversion efficiency (PCE) and fill factor (FF) shows a constant decline. The intrinsic carrier concentration (n_i) is directly proportional to temperature. As a result the reverse saturation current density (J_O) increases. This leads to enhanced charge recombination [30]. From

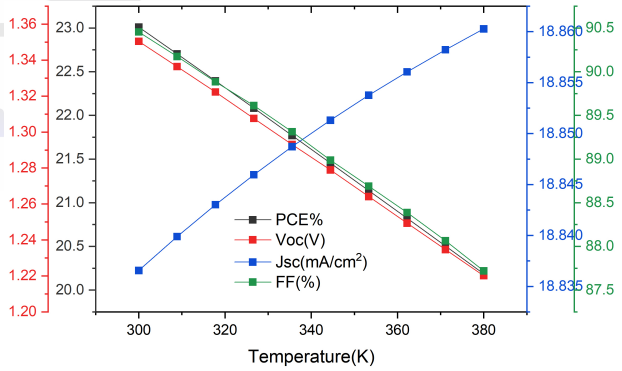

Fig. 8. Temperature dependence of photovoltaic parameters J_{SC}, V_{OC} FF, and PCE for the CdTe-based thin film solar cell under AM1.5G illumination.

© Ariston Publications 2026. All rights reserved.

the diode equation, the reverse saturation current J_O increases exponentially with temperature, which reduces V_{OC} as:

$$V_{oc} \approx \frac{kT}{q} \ln\left(\frac{J_{sc}}{J_0} + 1\right) \quad (10)$$

Where k is Boltzmann's constant, q is the elementary charge, T is temperature, J_o is the reverse saturation current and J_{SC} is the short-circuit current. The fill factor is strongly related with V_{OC} and internal series resistance. When V_{OC} decreases and thermal agitation increases recombination losses, as a result FF decreases [30].

The bandgap (Eg) of CdTe slightly get narrowed when we increase the temperature. A slightly smaller bandgap enables the solar cell to absorb slightly longer wavelengths of light. This leads to a marginal increase in J_{SC} [31].

The small gain in J_{SC} is far too minor to offset the significant reductions in V_{OC} and FF. As a result, overall Power Conversion Efficiency (PCE) declines as temperature goes up [29].

4.7 Impact of Temperature on J–V Characteristics of the Device

Figure 9 shows the J–V characteristics of the IGZO/CdTe/Cu_2O-based thin-film solar cell with different temperatures, namely, in the range from 300 K to 400 K.

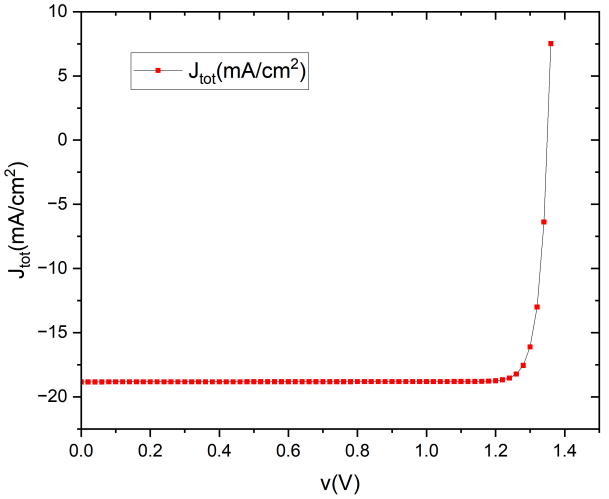

Fig. 9. Simulated J–V characteristics of the CdTe based Thin Film Solar Cell at different temperatures, showing degradation in output performance with increasing temperature.

The J–V characteristics have been simulated via SCAPS-1D simulator under standard AM1. 5G illumination. The J–V characteristics represent the plot between the total current density (J_{tot}) and voltage (V), depicting the effect of temperature on the electrical performance of the device [31]. With the increment in the working temperature, the position of J–V curve starts shifting gradually, indicating the change in charge transport properties of the device [11, 31]. At low voltage, the value of current density remains constant, but a drastic increase in the forward current density is seen when the applied voltage reaches the knee region. This indicates the occurrence of better carrier injection, which results in an increase in the reverse saturation current at high temperature, which is mainly due to the recombination process caused by temperature activation [11]. The open-circuit voltage (V_{oc}) gets decreased because of temperature elevation, and the slope of J–V curve around maximum power point becomes less steep [11, 30].

According to the diode equation, reverse saturation current (J_o) increases exponentially as the temperature increases, which causes the open-circuit voltage to decrease as follows:

$$V_{oc} \approx \frac{kT}{q} \ln\left(\frac{J_{sc}}{J_0} + 1\right) \quad (11)$$

where k is the Boltzmann constant, q is the electronic charge, T is the absolute temperature, Jo is the reverse saturation current, and J_{sc} is the short-circuit current.

From the above, it is clear that the J–V curve confirms that an increase in operating temperature negatively affects the electrical properties of the IGZO/CdTe/Cu_2O solar cell. Therefore, thermal stability is very important for CdTe-based thin-film solar cells [11, 31].

4.8 Study of Quantum Efficiency (QE) and Capacitance-Voltage (C–V) Characteristics

The quantum efficiency (QE) and Capacitive-Voltage (C-V) characteristics for the presented perovskite solar cell based on the PeDAMA$_3$ Pb_4I_{13} are shown in Figure 10 and 11, offering insights into their optical and electrical properties.

4.8.1 Quantum Efficiency Analysis:

The Quantum Efficiency (QE) curve is an indication of the capability of the solar cell in converting incident photons to charge carriers at various wavelengths. This also indicates the optical absorption and carrier collection efficiency [32]. For the simulated device, there is a high Quantum Efficiency of 88–90% for the range of wavelengths between 500–680 nm, showing that the photons

 © Ariston Publications 2026. All rights reserved.

are absorbed and charge carriers are extracted efficiently in the visible spectrum [32, 33]. Past 700 nm, the Quantum Efficiency drops sharply to nearly zero value at 720 nm, which corresponds to the cut-off wavelength due to the absorption limit of the absorber layer. This is because the cut-off wavelength depends on the absorber band gap (1.72–1.73 eV) for CdTe [5, 33].

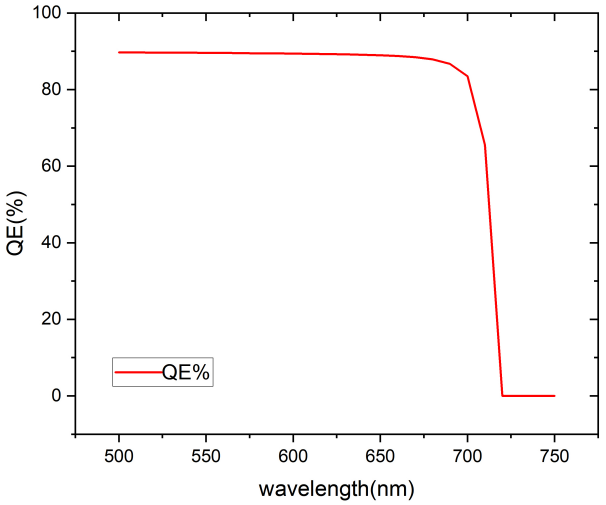

Fig. 10. Quantum Efficiency (QE) vs Wavelength of the CdTe based Thin Film Solar Cell.

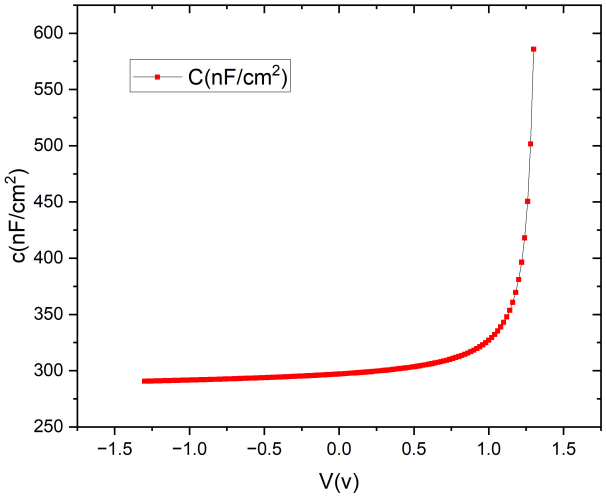

Fig. 11. Capacitance–Voltage (C–V) curve of the CdTe based Thin Film Solar Cell.

4.8.2 Capacitance/Voltage (C/V) Analysis

The graph shows how the capacitance varies in relation to the change in voltage in the range between −1.5 V and +1.3 V. The value of capacitance is relatively low and constant (280–300 nF/cm^2) as far as bias voltage is concerned in reverse and forward bias below 0.5 V. The above behavior is due to geometric capacitance and fully depletion of the junction wherein the depletion layer width does not vary much for low bias voltages [34, 35].

As the value of forward bias voltage increases beyond 0.8 V, there is a sudden rise in capacitance till it attains a value of 580–600 nF/cm^2 at 1.3 V. The above increase in capacitance is because of charge storage effect caused by carrier injection, diffusion capacitance, and accumulation of charge carriers in hetero-junction interface [34, 36].

From the above C-V characteristics, it can be seen that the control of the depletion width and the charge separation efficiency of the device is very good at low bias voltage, while there is improved charge injection at operating bias. Also, C-V characteristics may be studied by applying the Mott-Schottky equation to get the values of important electrical parameters like built-in potential and carrier concentration [34, 35].

5. CONCLUSION

A numerical study of a Front Contact / Cu_2O / CdTe / IGZO / Back Contact thin-film solar cell was conducted to analyze the impact of various parameters on photovoltaic efficiency. The variations in absorber thickness, transport layer thickness, defect density, series and shunt resistance, and the operating temperature were considered in order to find the best operational conditions of the investigated cell. According to the results of simulations, photovoltaic performance is dependent upon the combination of three phenomena, namely optical absorption, charge transport, and recombination. The use of an absorber thickness of 2.0 μm and the thickness of transport layers of 0.5 μm for both Cu_2O and IGZO ensured the best balance between light absorption and charge extraction. Lowering the defect density of the transport layers prevented the formation of recombination centers, while low series resistance and high shunt resistance decreased the electrical losses and improved the photovoltaic performance. At the same time, raising the temperature of operation from 300 K to 380 K resulted in a gradual decrease of V_{OC}, FF, and PCE due to increased recombination and reverse saturation current. The results showed that the developed device under optimized conditions attained a power conversion efficiency of 23.01% with open circuit voltage of 1.351 V, short circuit current density of 18.84 mA cm□² and fill factor of 90.46%. In general, this study proves that the simultaneous optimization of the material properties and the electrical parameters is vital for attaining the optimal performance of the CdTe thin-film solar cell.

© Ariston Publications 2026. All rights reserved.

DECLARATIONS

Ethical Approval

We affirm that this manuscript is an original work, has not been previously published, and is not currently under consideration for publication in any other journal or conference proceedings. All authors have reviewed and approved the manuscript, and the order of authoR$_{sh}$ip has been mutually agreed upon.

Funding

There are no funding

Availability of data and material

All of the data obtained or analyzed during this study is included in the report that was submitted.

Conflicts of Interest

The authors declare that they have no financial or personal interests that could have influenced the research and findings presented in this paper. The authors alone are responsible for the content and writing of this article.

Author's Contributions

All authors equally contributed

REFERENCES

[1] Haegel, N. M.; Atwater, H.; Barnes, T.; Breyer, C.; Burrell, A.; Chiang, Y. M.; others, **2019**. Terawatt-scale photovoltaics. *Science*, 364(6443), p.836--839. https://doi.org/10.1126/science.aaw1845.

[2] Green, M. A.; Dunlop, E. D.; Hohl-Ebinger, J.; Yoshita, M.; Kopidakis, N.; Bothe, K.; others, **2022**. Solar cell efficiency tables (Version 60). *Progress in Photovoltaics*, 30(7), p.687.

[3] Burgelman, M.; Nollet, P.; Degrave, S., **2000**. Modelling polycrystalline semiconductor solar cells. *Thin Solid Films*, 361, p.527--532. https://doi.org/10.1016/S0040-6090(99)00825-1.

[4] Poortmans, J.; Arkhipov, V., **2006**. Thin Film Solar Cells: Fabrication, Characterization and Applications. .

[5] Birkmire, R. W.; McCandless, B. E., **2010**. CdTe thin film technology: Leading thin film PV into the future. *Current Opinion in Solid State and Materials Science*, 14(6), p.139--142. https://doi.org/10.1016/j.cossms.2010.08.002.

[6] Yang, J. H.; Yin, W. J.; Park, J. S.; Ma, J.; Wei, S. H., **2016**. Review on first-principles study of defect properties of CdTe as a solar cell absorber. *Semiconductor Science and Technology*, 31(8), p.083002. https://doi.org/10.1088/0268-1242/31/8/083002.

[7] Chatterjee, S.; Pal, A. J., **2016**. Introducing Cu_2O thin films as a hole-transport layer in efficient planar perovskite solar cell structures. *The Journal of Physical Chemistry C*, 120(3), p.1428--1437. https://doi.org/10.1021/acs.jpcc.5b11540.

[8] Kamiya, T.; Hosono, H., **2010**. Material characteristics and applications of transparent amorphous oxide semiconductors. *NPG Asia Materials*, 2(1), p.15--22. https://doi.org/10.1038/asiamat.2010.5.

[9] Burgelman, M.; Verschraegen, J.; Degrave, S.; Nollet, P., **2004**. Modeling thin-film PV devices. *Progress in Photovoltaics: Research and Applications*, 12(2--3), p.143--153. https://doi.org/10.1002/pip.524.

[10] Easwarakhantan, T.; Nguyen, P. H.; Es-Slassi, A.; Ravelet, S., **1984**. Second-order effects of parasitic resistances on the efficiency of solar cells. *Solar Cells*, 13(1), p.77--82. https://doi.org/10.1016/0379-6787(84)90094-2.

[11] Kumar, S. G.; Rao, K. K., **2013**. Physics and chemistry of CdTe/CdS thin film heterojunction photovoltaic devices: Fundamental and critical aspects. *Energy & Environmental Science*, 7(1), p.45--102. https://doi.org/10.1039/C3EE41981A.

[12] Zuo, C.; Ding, L., **2015**. Solution-Processed Cu_2O and CuO as Hole Transport Materials for Efficient Perovskite Solar Cells. *Small*, 11(41), p.5528--5532. https://doi.org/10.1002/smll.201501330.

[13] Ravindra, P.; Mukherjee, R.; Avasthi, S., **2017**. Hole-selective electron-blocking copper oxide contact for silicon solar cells. *IEEE Journal of Photovoltaics*, 7(5), p.1278--1283. https://doi.org/10.1109/JPHOTOV.2017.2720619.

 © Ariston Publications 2026. All rights reserved.

[14] Rao, Z.; Du, B.; Huang, C.; Shu, L.; Lin, P.; Fu, N.; Ke, S., **2019**. Revisit of amorphous semiconductor $InGaZnO_4$: A new electron transport material for perovskite solar cells. *Journal of Alloys and Compounds*, 789, p.276--281. https://doi.org/10.1039/C3EE41981A.

[15] Nomura, K.; Ohta, H.; Takagi, A.; Kamiya, T.; Hirano, M.; Hosono, H., **2004**. Room-temperature fabrication of transparent flexible thin-film transistors using amorphous oxide semiconductors. *Nature*, 432(7016), p.488--492. https://doi.org/10.1038/nature03090.

[16] Chowdhury, M. S.; Shahahmadi, S. A.; Chelvanathan, P.; Tiong, S. K.; Amin, N.; Techato, K. A.; others, **2020**. Effect of deep-level defect density of the absorber layer and n/i interface in perovskite solar cells by SCAPS-1D. *Results in Physics*, 16, p.102839. https://doi.org/10.1016/j.rinp.2019.102839.

[17] Cheragee, S. H.; Alam, M. J., **2023**. Device modeling and numerical study of a double absorber solar cell using a variety of electron transport materials. *Heliyon*, 9(7). https://doi.org/10.1016/j.heliyon.2023.e18265.

[18] Medina, J. C. Z.; Andrés, E. R.; Ruíz, C. M.; Espinosa, E. C.; Yarce, L. T.; Isasmendi, R. G.; others, **2023**. Performance simulation of solar cell based on AZO/CdTe heterostructure by SCAPS 1D software. *Heliyon*, 9(3). https://doi.org/10.1016/j.heliyon.2023.e14547.

[19] Putra, N. M. D.; Marwoto, P.; Murtafiatin, R.; Permadis, D. P., **2021**. The SCAPS-1D modeling of ZnO/CdS/CdTe thin film: Analysis of thickness and stoichiometric fraction of absorber layer on solar cell performance. , 1918(2). https://doi.org/10.1088/1742-6596/1918/2/022029.

[20] Johora, F. T.; Khan, M. A.; Al Asad, A.; Islam, M. R.; Rayhan, A., **2024**. Effect of Defect Density Variation in CdTe Solar Cell Using Cu as A Hole Transport Layer and Back Contact. *International Journal of Electrical Engineering and Applied Sciences (IJEEAS)*, 7(2). https://doi.org/10.54554/ijeeas.2024.7.02.009.

[21] Shockley, W.; Read, W. T., **1952**. Statistics of the recombinations of holes and electrons. *Physical Review*, 87(5), p.835. https://doi.org/10.1103/PhysRev.87.835.

[22] Hossain, M. K.; Rubel, M. H. K.; Toki, G. I.; Alam, I.; Rahman, M. F.; Bencherif, H., **2022**. Effect of various electron and hole transport layers on the performance of $CsPbI_3$-based perovskite solar cells: A numerical investigation in DFT, SCAPS-1D, and wxAMPS frameworks. *ACS Omega*, 7(47), p.43210--43230. https://doi.org/10.1021/acsomega.2c05912.

[23] Jain, S. K.; Sharma, G.; Vyas, S., **2023**. Influence of hole interface layer on the performance of cadmium telluride-based thin film solar cell. *Materials Today: Proceedings*, 74, p.231--233. https://doi.org/10.1016/j.matpr.2022.08.058.

[24] Yang, J. H.; Metzger, W. K.; Wei, S. H., **2017**. Carrier providers or carrier killers: The case of Cu defects in CdTe solar cells. *arXiv preprint arXiv:1701.06068*. https://doi.org/10.48550/arXiv.1701.06068.

[25] Harif, M. N.; Doroody, C.; Nadzri, A.; Rosly, H. N.; Ahmad, N. I.; Isah, M.; Amin, N., **2023**. Effect of Cu_2Te back surface interfacial layer on cadmium telluride thin film solar cell performance from numerical analysis. *Crystals*, 13(5), p.848. https://doi.org/10.3390/cryst13050848.

[26] Carranza, A. C.; Rosendo, E.; Zepeda, J. C.; Morales, C.; Camacho, E.; Treviño, L.; others, **2026**. Theoretical Optimization of Environmentally Friendly Alternative Indium-Doped Zinc Oxide (IZO) in CdTe Solar Cell Technology by SCAPS-1D. *Transactions on Electrical and Electronic Materials*, 27(3), p.510--522. https://doi.org/10.1007/s42341-025-00680-2.

[27] Song, T.; Kanevce, A.; Sites, J. R., **2016**. Emitter/absorber interface of CdTe solar cells. *Journal of Applied Physics*, 119(23). https://doi.org/10.1063/1.4953820.

[28] Montoya De Los Santos, I.; Pérez-Orozco, A. A.; Liña-Martínez, D. A.; Courel, M.; Meza-Avendaño, C. A.; Borrego-Pérez, J. A.; others, **2023**. Towards a CdTe solar cell efficiency promotion: The Role of ZnO:Al and CuSCN nanolayers. *Nanomaterials*, 13(8), p.1335. https://doi.org/10.3390/nano13081335.

[29] Romeo, A.; Artegiani, E., **2021**. CdTe-based thin film solar cells: Past, present and future. *Energies*, 14(6), p.1684. https://doi.org/10.3390/en14061684.

© Ariston Publications 2026. All rights reserved.

[30] Singh, P.; Ravindra, N. M., **2012**. Temperature dependence of solar cell performance---an analysis. *Solar Energy Materials and Solar Cells*, 101, p.36--45. https://doi.org/10.1016/j.solmat.2012.02.019.

[31] Fonthal, G.; Tirado-Mejía, L.; Marín-Hurtado, J. I.; Ariza-Calderón, H.; Mendoza-Alvarez, J. G., **2000**. Temperature dependence of the band gap energy of crystalline CdTe. *Journal of Physics and Chemistry of Solids*, 61(4), p.579--583. https://doi.org/10.1016/S0022-3697(99)00254-1.

[32] Nakane, A.; Tampo, H.; Tamakoshi, M.; Fujimoto, S.; Kim, K. M.; Kim, S.; others, **2016**. Quantitative determination of optical and recombination losses in thin-film photovoltaic devices based on external quantum efficiency analysis. *Journal of Applied Physics*, 120(6). https://doi.org/10.1063/1.4960698.

[33] Jiang, Y.; Hu, D.; Tang, P.; Zhang, J.; Liu, C.; Wang, W.; others, **2017**. A study of apparent quantum efficiency in different structures of cadmium telluride solar cells. *Solar Energy*, 149, p.323--331. https://doi.org/10.1016/j.solener.2017.03.085.

[34] Werner, F.; Babbe, F.; Elanzeery, H.; Siebentritt, S., **2019**. Can we see defects in capacitance measurements of thin-film solar cells?. *Progress in Photovoltaics: Research and Applications*, 27(11), p.1045--1058. https://doi.org/10.1002/pip.3196.

[35] Li, J. V.; Halverson, A. F.; Sulima, O. V.; Bansal, S.; Burst, J. M.; Barnes, T. M.; others, **2012**. Theoretical analysis of effects of deep level, back contact, and absorber thickness on capacitance--voltage profiling of CdTe thin-film solar cells. *Solar Energy Materials and Solar Cells*, 100, p.126--131. https://doi.org/10.1016/j.solmat.2012.01.003.

[36] Gudovskikh, A. S.; Chouffot, R.; Kleider, J. P.; Kaluzhniy, N. A.; Lantratov, V. M.; Mintairov, S. A.; others, **2008**. New method for interface characterization in heterojunction solar cells based on diffusion capacitance measurements. *Thin Solid Films*, 516(20), p.6786--6790. https://doi.org/10.1016/j.tsf.2007.12.021.

ARISTON PUBLICATIONS

 © Ariston Publications 2026. All rights reserved.